Available online at www.sciencedirect.com
SCIENCE DIRECT®
ELSEVIER
Nuclear Instruments and Methods in Physics Research B 199 (2003) 174–178
NIM B
Beam Interactions with Materials & Atoms
www.elsevier.com/locate/nimb

Local structure of Ge/Si nanostructures: Uniqueness of XAFS spectroscopy

A.V. Kolobov [a,*,1], H. Oyanagi [b], A. Frenkel [c], I. Robinson [d], J. Cross [e], S. Wei [f], K. Brunner [g], G. Abstreiter [g], Y. Maeda [h], A. Shklyaev [i], M. Ichikawa [i], S. Yamasaki [a], K. Tanaka [i]

[a] *National Institute of Advanced Industrial Science and Technology (AIST) – Joint Research Center for Atom Technology (JRCAT), 1-1-1 Higashi, Tsukuba, Ibaraki 305-8562, Japan*
[b] *AIST, 1-1-1 Umezono, Tsukuba, Ibaraki 305-8568, Japan*
[c] *Department of Physics, Yeshiva University, New York, NY 10016, USA*
[d] *University of Illinois at Urbana-Champaign, Urbana, IL 61801, USA*
[e] *PNC-CAT, Argonne National Laboratory, Argonne, IL 60439, USA*
[f] *National Synchrotron Radiation Laboratory, University of Science and Technology of China, Hefei 230029, China*
[g] *Walter Schottkey Institute, TU Munich, Garshing 85748, Germany*
[h] *Osaka Prefecture University, Osaka 599-8531, Japan*
[i] *Angstrom Technology Partnership (ATP), Tsukuba, Ibaraki 305-0046, Japan*

Abstract

A discussion of the limitations of Raman scattering as applied to Ge/Si nanostructures is followed by a summary of our recent efforts to investigate the local structure of various Ge nanostructures, namely, Ge quantum dots MBE grown on bare Si(1 0 0), on Si(1 1 1) with a 0.3 nm SiO_2 coverage, and nanocrystals embedded in SiO_2, by X-ray absorption fine structure spectroscopy. For the latter case, combined DAFS–EXAFS analysis has been applied to determine separately, for the first time, the structural parameters for intermixed nanocrystalline and amorphous phases.

PACS: 61.10.Ht; 68.65.+g
Keywords: Ge nanostructures; Quantum dots; Nanocrystals; Raman scattering; EXAFS; DAFS

1. Introduction

Recent years have witnessed growing interest in nanometer-scale semiconductor structures. A technique to fabricate such nanostructures is epitaxial growth when the lattice mismatch between the substrate and the overgrown layer allows the formation of self-assembled quantum dots (QDs) through the Stranski–Krastanov mechanism [1]. Another method consists in the formation of semiconductor nanocrystals embedded in an insulating matrix [2]. Interest in Si and Ge nanostructures is additionally driven by the conjecture that in small-size particles the efficiency of optical

* Corresponding author. Fax: +81-298-612 939.
E-mail address: a.kolobov@aist.go.jp (A.V. Kolobov).
[1] On leave from A.F. Ioffe Physico-Technical Institute, St. Petersburg, Russia.

0168-583X/02/$ - see front matter
PII: S0168-583X(02)01556-2

transitions may be increased by orders of magnitude [3].

Atomic force microscopy (AFM) or transmission electron microscopy (TEM) are often used to characterize the grown samples. These techniques allow one to determine the size and shape of the nanostructures but not their local structure. For the latter purpose, Raman scattering is often used. In the particular case of Ge/Si nanostructures, however, it often fails to provide unambiguous information because the Raman signal is dominated by replicas of the photon density of states of the Si substrate [4].

An alternative technique for determination of the local structure is X-ray absorption fine structure (XAFS) spectroscopy. In this paper we demonstrate its successful application to different Ge nanostructures, namely, Ge QDs grown on Si(1 0 0) by molecular beam epitaxy (MBE), Ge nanocrystals embedded in SiO_2, and Ge nanoislands formed on Si(1 1 1) with a thin SiO_2 coverage.

For the case of embedded nanocrystals, we found that Ge co-exists in two phases – nanocrystalline and amorphous – and we have applied diffraction anomalous fine structure (DAFS) in order to characterize separately the structure of each phase. To the best of our knowledge this is the first direct determination of the local structure of the amorphous phase in presence of the crystalline phase of the same material.

2. Experimental details

XAFS measurements have been performed at BL13B of the Photon Factory. The measurements were done at room temperature using a grazing-incidence geometry in fluorescence mode. See [5] for more details. For the data analysis, we have performed the curve-fitting for a region typically extending from 3 to 16 $Å^{-1}$ using the FEFFIT code of UWXAFS3.0 [6]. Theoretical backscattering amplitudes and phase shifts were calculated using FEFF8 [7].

The DAFS experiment was performed at room temperature using a custom-designed 4-circle Kappa diffractometer at the National Synchrotron Light Source at Brookhaven National Laboratory, beamline X16C. The (1 1 1) reflection has been used for the experiment. More details on the equipment can be found in [8].

3. Results and discussion

3.1. Ge/Si self-assembled quantum dots

The samples were grown by MBE on Si(1 0 0) substrates at three different temperatures of 510, 550 and 745 °C and were capped by ~50 nm Si [1].

Fig. 1 shows raw EXAFS oscillations for QDs grown at 745 °C. Shown for comparison are EXAFS oscillations for bulk Ge and for a solid solution of Ge in Si ($Ge_{0.006}Si_{0.994}$). The very strong resemblance of the raw EXAFS oscillations of the

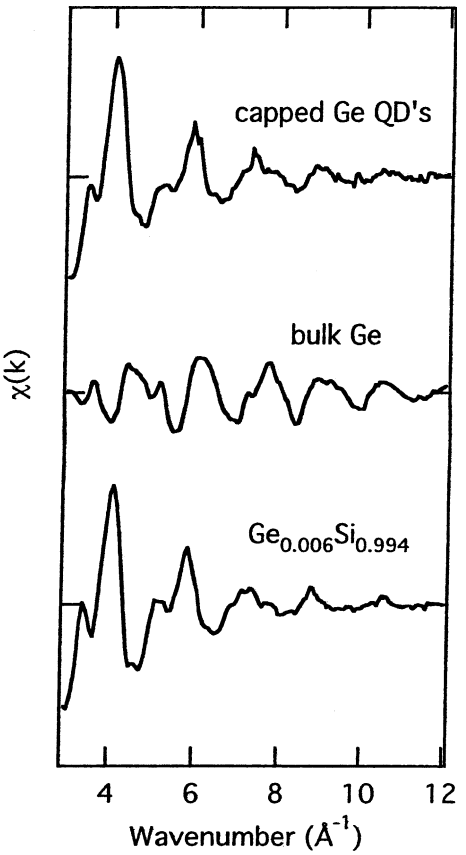

Fig. 1. Raw EXAFS oscillations for Ge/Si(1 0 0) QDs grown at 745 °C together with EXAS spectra for bulk c-Ge and a dilute solid solution $Ge_{0.006}Si_{0.994}$.

Table 1
Fitting results for Si-capped Ge/Si(1 0 0) QDs

Growth T	N_{GeSi}	BL_{GeGe} Å	BL_{GeSi} Å
510 °C	2.7 ± 0.1	2.42 ± 0.01	2.37 ± 0.01
550 °C	2.9 ± 0.1	2.41 ± 0.01	2.38 ± 0.01
745 °C	3.9 ± 0.3		2.37 ± 0.01

QDs with those of the solid solution, provides by itself sufficient grounds to claim that Ge is strongly intermixed with silicon. To get quantitative results, we have fitted the first peak with both Ge–Ge and Ge–Si correlations. The obtained Ge–Si partial coordination number is 3.9 ± 0.3. The uncertainty does not allow us to completely exclude the presence of the Ge phase. However, the obtained values do allow us to claim that the fraction of Ge existing as pure Ge phase is less that 10% of the total amount.

A summary of the results is given in Table 1. One can see that the fraction of the Ge phase increases when the growth temperature decreases. Taking into account the fact that about 60% of Ge is within the wetting layer and assuming that the wetting layer intermixes with Si more efficiently that the dots, we can conclude that the QDs grown at lower temperature consist of Ge-rich phase. This result agrees with the results of independent XANES analysis [9] and recent findings of other authors [10].

For the sample which do possess the Ge phase (510 and 550 °C) we have also performed polarised XAFS studies (measured at BL12C at the Photon Factory [11]). We found that their structural parameters were identical for the two polarisations (within the error bars of ±0.02 Å). From this result we conclude that the strain in the Ge-rich phase is accommodated by the bond angles rather than by the bond lengths.

In the case of uncapped Ge QDs we have found that Ge is partly oxidized and partly alloyed with Si. For the growth temperature of 745 °C the fraction of each phase is about 30% each [9].

3.2. Embedded Ge nanocrystals

The samples were prepared by co-deposition of Ge- and Si-oxides by radio-frequency (rf) magnetron sputtering. The Ge concentration varied from 25 to 60 mol.%. After the deposition, the samples were annealed for 1 h at 800 °C in an argon atmosphere which produced nanocrystals with a typical size of 5–20 nm [2].

We found that in as-made samples with low and intermediate Ge content, Ge was predominantly coordinated by oxygen atoms while in the sample with 60 mol.% Ge, Ge–Ge correlations are also present. Upon annealing, a peak corresponding to the second-nearest Ge–Ge correlations appears (Fig. 2), which demonstrates the formation of the Ge crystalline phase. For the nanocrystals formed in the 60 mol.% Ge sample we obtained the Ge–Ge bond length of 2.45 ± 0.02 Å. From an analysis of the second Ge–Ge peak we found that the fraction of Ge atoms in the nc-Ge phase is found to be ~50%. Full details of the EXAFS data analysis will be published elsewhere [12].

In order to separate the contribution from the nanocrystalline and amorphous phases, we have carried out DAFS measurements (Fig. 3). The $f''(E)$, which is related to the absorption cross-section $\sigma(E)$ by the optical theorem, was isolated using the iterative dispersion integral algorithm [13] and is shown in the insert. The EX-

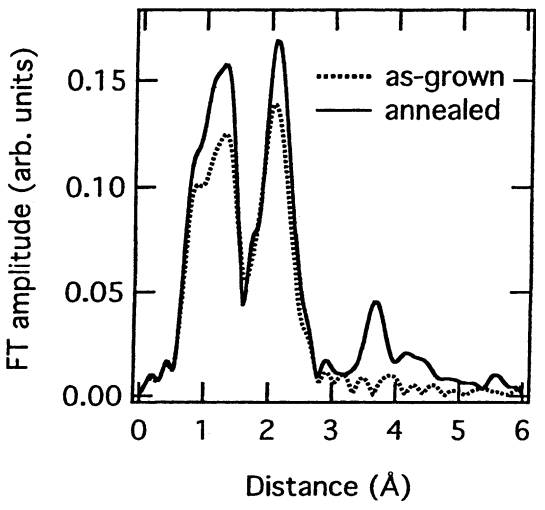

Fig. 2. Magnitudes of Fourier transforms for the as-grown and annealed samples with 60 mol.% Ge (quartz–glass substrate). Appearance of higher shell upon annealing evidences the formation of the crystalline phase.

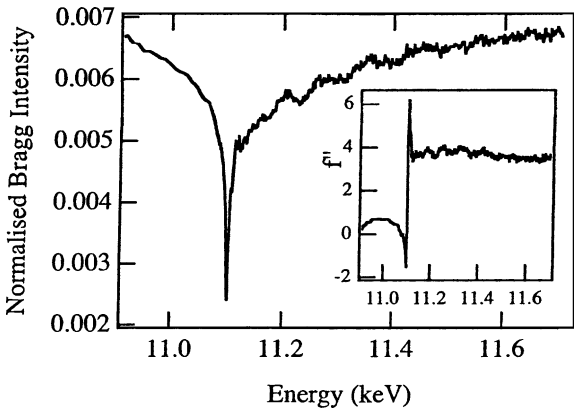

Fig. 3. A DAFS spectrum [(1 1 1) reflection] for a sample containing a mixture of nanocrystalline and amorphous Ge.

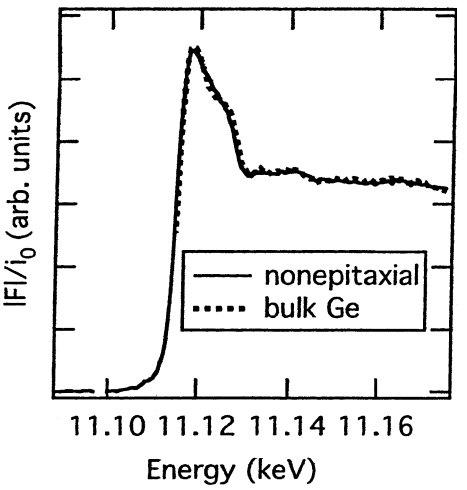

Fig. 4. A XANES spectrum for the non-epitaxial Ge islands.

AFS signal $\chi(k)$ obtained from f'' originates from the nanocrystalline Ge phase (nc-Ge) only. The nc-Ge–Ge distance obtained was 2.44 ± 0.02 Å. By combining the DAFS-extracted EXAFS signal of the nc-Ge phase and the cumulative signal containing a mixture of GeO, a-Ge and nc-Ge, we could reliably deconvolute the structural contributions of all three phases by repeating the fitting procedure to fit the total Ge EXAFS signal with the Ge–O, a-Ge–Ge distances, their disorders and coordination numbers being independently varied, while the distances and their disorders in the nc-Ge–Ge phase were fixed to be the same as obtained in the previous DAFS analysis. The Ge–Ge bond length in a-Ge was found to be 2.50 ± 0.03 Å. This value is in agreement with the result obtained for disordered Ge nanoislands [14].

Whilst discrimination between structural contributions to the EXAFS signal in the mixture of crystalline and amorphous phases of the same element have been attempted in the past [15] it is only with DAFS–EXAFS combination used in this work that we were able, for the first time, to measure the structural contribution of the nanocrystalline and amorphous states of the same element directly.

3.3. Ge nanoislands on oxidized Si(1 1 1)

Recently, it was reported [16] that growth of Ge islands on a Si(1 1 1) surface with a thin SiO_2 coverage resulted in the formation of ultra-small islands with a hemispherical shape, typically less than 7 nm in base diameter and 2.5 nm in height. Depending on the growth temperature, the nanoislands can be either epitaxial or non-epitaxial with respect to the substrate.

Fig. 4 shows XANES spectra for the non-epitaxial Ge islands (the grown samples were kept in atmosphere for three months prior to the measurements). One can see from the figure that the non-epitaxial islands (1) preserve the structure of bulk Ge without intermixing with Si and (2) they are very stable against oxidation at room temperature. We have additionally found [17] that the non-epitaxial islands exhibit a broad photoluminescence peak located at ~2.3 eV. The epitaxial islands were found to be partially oxidized and partially alloyed with Si.

4. Conclusions

Our results demonstrate that Raman scattering should be applied to Ge/Si nanostructures with extreme care. The technique of choice for this system is XAFS. Our results obtained on differently grown nanostructure show that the local structure of Ge varies, depending on the preparation technique, from the bulk Ge structure to a very dilute solid solution in Si. Application of

combined DAFS–EXAFS analysis allowed us to separate the structural parameters of the intermixed nanocrystalline and amorphous phases.

Acknowledgements

This work was partly supported by NEDO and the European Community (MEL-ARI project SIBOIA No 28824) and was performed at JRCAT under a research agreement between AIST and ATP.

References

[1] P. Schnittenhelm, M. Gail, J. Brunner, J.F. Nutzel, G. Abstreiter, Appl. Phys. Lett. 67 (1995) 1292.
[2] Y. Maeda, Phys. Rev. B 51 (1995) 1658.
[3] T. Takagahara, K. Takeda, Phys. Rev. B 46 (1992) 15578.
[4] A.V. Kolobov, J. Appl. Phys. 87 (2000) 2926.
[5] H. Oyanagi, R. Shioda, Y. Kuwahara, K. Haga, J. Synchr. Rad. 2 (1995) 99.
[6] M. Newville, P. Livins, Y. Yacoby, J.J. Rehr, E. Stern, Phys. Rev. B 47 (1993) 14126.
[7] A. Ankudinov, B. Ravel, J.J. Rehr, S.D. Conradson, Phys. Rev. B 58 (1998) 7565.
[8] J.O. Cross, A.I. Frenkel, Rev. Sci. Instr. 70 (1999) 38.
[9] A.V. Kolobov, H. Oyanagi, K. Brunner, P. Schittenhelm, G. Abstreiter, K. Tanaka, Appl. Phys. Lett. 86 (2001) 451.
[10] G. Capellini, M.D. Seta, F. Evangelisti, Appl. Phys. Lett. 78 (2001) 303.
[11] M. Nomura, A. Koyama, KEK Report 95-15, 1996.
[12] A.V. Kolobov, S. Wei, W. Yan, H. Oyanagi, Y. Maeda, in press.
[13] J.O. Cross, Ph.D. Thesis, University of Washington, Seattle, 1996.
[14] A.V. Kolobov, H. Oyanagi, A.A. Shklyaev, S. Yamasaki, M. Ichikawa, in: Proc. 6th Int. Symp. on Advanced Physical Fields, Tsukuba, 2001, p. 162.
[15] E.A. Stern, C.E. Bouldin, B. von Roedern, J. Azoulay, Phys. Rev. B 27 (1983) 6557.
[16] A.A. Shklyaev, M. Shibata, M. Ichikawa, Phys. Rev. B 62 (2000) 1540.
[17] A.V. Kolobov, A.A. Shklyaev, H. Oyanagi, P. Fons, S. Yamasaki, M. Ichikawa, Appl. Phys. Lett. 78 (2001) 2563.